2014-06-01

Understanding the Benefits and Limitations of Increasing Maximum Rotor Tip Speed for Utility-Scale Wind Turbines

Andrew Ning
Brigham Young University - Provo, aning@byu.edu

Understanding the Benefits and Limitations of Increasing Maximum Rotor Tip Speed for Utility-Scale Wind Turbines

A Ning[1] **and K Dykes**[2]

[1] Senior Engineer, National Renewable Energy Laboratory, Golden, CO
[2] Research Analyst, National Renewable Energy Laboratory, Golden, CO

E-mail: andrew.ning@nrel.gov

Abstract. For utility-scale wind turbines, the maximum rotor rotation speed is generally constrained by noise considerations. Innovations in acoustics and/or siting in remote locations may enable future wind turbine designs to operate with higher tip speeds. Wind turbines designed to take advantage of higher tip speeds are expected to be able to capture more energy and utilize lighter drivetrains because of their decreased maximum torque loads. However, the magnitude of the potential cost savings is unclear, and the potential trade-offs with rotor and tower sizing are not well understood. A multidisciplinary, system-level framework was developed to facilitate wind turbine and wind plant analysis and optimization. The rotors, nacelles, and towers of wind turbines are optimized for minimum cost of energy subject to a large number of structural, manufacturing, and transportation constraints. These optimization studies suggest that allowing for higher maximum tip speeds could result in a decrease in the cost of energy of up to 5% for land-based sites and 2% for offshore sites when using current technology. Almost all of the cost savings are attributed to the decrease in gearbox mass as a consequence of the reduced maximum rotor torque. Although there is some increased energy capture, it is very minimal (less than 0.5%). Extreme increases in tip speed are unnecessary; benefits for maximum tip speeds greater than 100-110 m/s are small to nonexistent.

1. Introduction

The maximum rotational speed of utility-scale wind turbines is often limited by noise considerations. Aerodynamic blade noise is generally one of the largest acoustic emissions from a wind turbine, and the magnitude of that noise is strongly dependent on the tip speed of the blades [1]. Improvements in detailed shape design, acoustic shielding, site layout, and siting at remote and offshore locations enable the possibility of operating wind turbines at higher maximum tip speeds. The expected benefits of turbines designed to operate at higher tip speeds are increased energy capture at the top of Region 2 and decreased maximum torque loads that lead to lighter drivetrains. However, the increase in the rotor rotational frequency and a potential increase in peak thrust loads may require heavier main bearings and a stiffer tower. The trade-offs between power capture and capital costs require an integrated assessment of an entire wind turbine and site.

This study is not concerned with turbine design optimization for the purpose of noise reduction. Many studies exist exploring this theme [2–4]. Rather, we seek to quantify the non-acoustic benefits of increasing rotor tip speed to better assess whether the concept justifies increased research and investment in noise-mitigation strategies. A study by Jamieson suggests that a 15%–20% reduction in turbine capital costs is possible for a flexible downwind configuration with very high tip speeds [5]. A precursor study done by the National Renewable

Energy Laboratory (NREL) and Sandia National Laboratories was recently completed using a sequential optimization process for a wind turbine in which the rotor was first optimized, the nacelle and tower were subsequently optimized, and a cost-of-energy analysis was performed for the overall system [6, 7]. This study estimated that up to a 3% reduction in the cost of energy was possible when an optimized point design at a 100-m/s tip-speed limit was compared to a baseline optimized design at an 80-m/s limit. The sequential nature of the optimization, and the use of different objectives in each subsystem optimization, left questions about how the results might vary when viewed as a system-level optimization problem.

To address these limitations, this study uses an integrated modeling tool, the Wind-Plant Integrated Systems Design and Engineering Model (WISDEM), to perform a system-level nonlinear optimization on a wind turbine with the wind plant's cost of energy as the overall system objective. Using an integrated model set with combined physics and cost modeling capabilities allows for the direct exploration of trade-offs in the design of different subsystems. In addition, the study moves beyond a single-point comparison to consider system optimization over a range of tip speeds, for a variety of different wind plant site conditions, and with added degrees of freedom for rotor diameter and hub height. All of this leads to additional insight into potential cost-of-energy reductions by relaxing maximum tip-speed constraints in the design of wind turbines.

2. Methodology

The methodology builds upon that described in [8–10]. Rotor aerodynamic performance was estimated using blade element momentum theory with a novel solution approach that enables usage in gradient-based optimization applications [11], and blade structural analysis was done using beam finite element theory and classical laminate theory. Tower aerodynamics and hydrodynamics were based on a power-law wind profile, linear wave theory, and cylinder drag, while the tower structural analysis was based on beam finite element theory, a shell buckling estimation method from Eurocode 3 [12], and a global buckling estimation method from GL [13]. For both the rotor and tower, FAST [14] aeroelastic simulations were performed prior to optimization to estimate damage equivalent moments along the tower and blades. Because of the significant computational costs, FAST was not used during the optimization. The changes in geometry and stiffness were used in computing the corresponding stress and damage, but with the assumption that the rainflow-cycle counted bending moments would not change appreciably during the optimization. This assumption was found to hold reasonably well for designs that were rechecked in FAST post-optimization. Certainly, this type of constraint is not a replacement for a full fatigue analysis, but can be useful for conceptual design purposes, particularly in this study where buckling, and stiffness related criteria were more dominant constraints compared to that of fatigue.

Critical to this study was the development of a physics-based hub and drivetrain component model set for performance analysis under various extreme load conditions [15]. One of the main advantages for increased tip speed is the reduction of peak torque loads. This is expected to allow for a significant size reduction in drivetrain mass and costs. The model uses a four-point suspension design (two main bearings) with a three-stage gearbox. Using bearing positions, and the low-speed shaft geometry and material composition, the model analyzes shaft deflection behavior as well as loads on the bearings and shaft. Smoothing functions of real bearing data by type is used for load capacity and dimensioning. The bedplate is modeled as a pair of I-beams with a multiplier to account for additional front frame support weight based on higher-fidelity model data. Finally, the hub and yaw system are sized based on rotor loads and diameter, respectively. More details on the drivetrain models can be found in [15].

The overall optimization objective is based on wind plant cost of energy. In this case, financing aspects are ignored and the cost of energy is calculated via the formula:

$$COE = \frac{FR(TCC + BOS) + (1 - T)OPEX}{AEP} \tag{1}$$

Where COE is the project levelized cost of energy, TCC is the total turbine capital costs for the

project, BOS is the total balance of station costs for the project, OPEX is the overall project operational expenditures, AEP is the annual energy production, FR is the financing rate, and T is the tax deduction rate on OPEX (fixed at 0.095 and 0.4 respectively, as used in [16]).

For this analysis, simplified models were used for the nonturbine cost elements of COE. The NREL Cost and Scaling Model (CSM) [17] was used for the offshore BOS and OPEX. The NREL CSM OPEX model depends primarily on machine rating and AEP but also sea depth for offshore projects. Offshore BOS costs in the NREL CSM model depend only on machine rating (which does not vary in the study), rotor diameter, hub height, and sea depth. In addition, the costs of this model are known to significantly underpredict BOS costs compared to those of realistic projects, and a factor of 2.33 was used to bring the costs into better alignment with typical costs for a commercial project, at $3,650 USD/kW [16]. For the land-based BOS, a newly developed model at NREL was available that predicts much more realistic costs for BOS than those of the NREL CSM. However, even using the new model, costs were much lower than those estimated in [16] for land-based per-kW balance-of-station costs ($620 USD/kW) and a multiplier of 2.23 was used to bring the model estimate of $278 USD/kW up to more realistic costs. The model is undergoing development and has not yet been published but was used here because of the aforementioned limitations of the NREL CSM BOS model.

A new model was used for turbine capital cost analysis in which the cost of each component was determined as a function of its mass and the overall turbine cost accounted for manufacturing assembly, transport, overhead, and adders for profit [18]. The component mass-cost relationships were based on the data underlying the NREL CSM and are updated as new turbine component cost data is available. Thus, as the turbine design changes with each iteration, the component masses are updated, which in turn changes the overall TCC.

For the overall system model, the above models were all linked together into the new Wind-Plant Integrated Systems Design & Engineering Model (WISDEM) [10]. WISDEM is developed in OpenMDAO, a Python-based framework for multidisciplinary analysis and optimization [19]. The rotor, hub, nacelle, drivetrain, and tower models are all linked together into a turbine design model in which the design variables and constraints can be applied to any of the subsystem variables. These models are all linked to the turbine and plant cost models to allow for full system cost-of-energy analysis.

Although analytic gradients were derived for almost all of the modules, system gradients were instead estimated using finite differencing. Using mixed derivatives (some analytic, some finite differenced) led to performance issues that had not yet been addressed at the time of this writing. However, it was found that because all modules were written with differentiability in mind, finite differencing was accurate, robust, and fast enough for the problems considered here. All optimization problems were solved using SNOPT, a software package for solving large-scale optimization problems using a sequential quadratic programming method [20]. The design variables and constraints for the optimization are summarized in Table 1 and Table 2.

Distributions, such as the blade chord distribution, were parameterized with a small number of variables and fit with an Akima spline to define chord lengths along the entire blade. For all loading conditions, standard IEC safety factors were applied [21]. The worst-case ultimate loading for the rotor was assumed to occur at the survival wind speed with a blade pitch failure. For the tower, both the survival wind speed and the maximum thrust condition were used. Additional bound constraints for maximum blade chord were used because of transportation limitations. Some of the rotor and tower constraints, such as ultimate strain, were imposed only at a subset of the stations because they varied continuously and including all stations was unnecessary. More details on the optimization setup can be found in [8] and [9].

2.1. Reference Turbines and Wind Projects

In performing an optimization for a turbine and plant, a reference project is needed that defines the main turbine and plant features. In this case, the NREL 5-MW reference turbine [22] was used as the reference turbine for each project. This model has been used for various wind energy research analyses in the past, and a drivetrain model for the turbine was recently created using the hub, nacelle, and drivetrain models described above [15].

Table 1. Design variables used in optimization.

Component	Description	# of variables
rotor	chord distribution	5
rotor	twist distribution	4
rotor	spar-cap thickness distribution	5
rotor	trailing-edge panel thickness distribution	5
rotor	tip-speed ratio in Region 2	1
rotor	diameter	1
nacelle	shaft lengths in low-speed shaft	2
nacelle	bedplate I-beam sizing	2
tower	diameters	3
tower	wall thicknesses	3
tower	waist location	1
tower	height	1
monopile	diameter	1
monopile	wall thickness	1

Table 2. Nonlinear constraints used in optimization.

Component	Description	# of constraints
rotor	ground strike and tower strike	2
rotor	resonance avoidance	2
rotor	ultimate strain in spar-cap and trailing-edge	24
rotor	panel buckling in spar-cap and trailing-edge	14
rotor	fatigue damage	10
nacelle	deflection limits in low-speed shaft	4
nacelle	deflection limits in bedplate	2
nacelle	ultimate stress in bedplate	2
tower	ultimate stress	14
tower	fatigue damage	9
tower	buckling (shell and global)	28
tower	resonance avoidance	1
tower	diameter-to-thickness ratio	1
tower	taper ratio	1
monopile	ultimate stress	2
monopile	buckling	2
monopile	diameter-to-thickness ratio	2

Three reference project wind plants were used in the study: a land-based high-wind-speed site (IEC Class IB), a land-based low-wind-speed site (IEC Class IIIB), and an offshore high-wind-speed site (IEC Class IB). Site characteristics came from standard IEC specifications [12], with the offshore site using a lower shear factor [23]. The offshore site was also assumed to have a sea depth of 20 m.

Because the NREL 5-MW reference turbine was designed for offshore applications its direct use for a land-based site is challenging. Transportation limitations over land would restrict tower diameters to about 4.6 m. At those diameters, extreme wall thicknesses would be required for 5-MW turbines that utilize steel tubular towers. Due to a lack of detailed models for other multimegawatt reference turbines and novel tower technologies, the NREL 5-MW reference model was still used in the land-based studies, but the tower transportation constraint was ignored.

3. Results

To understand the impact of tip speed on wind turbine design, a series of optimizations were performed, each with a different constraint on the maximum tip speed. It is important to note that the rotor was not forced to actually operate up to the maximum tip speed; rather, it was simply prevented from exceeding that limit. The studies in this section are separated into three main themes. First, the trends in cost and mass as a function of tip speed are examined for a high-wind-speed land-based site. Second, the trends in cost of energy are compared to a low-wind-speed land-based site and a high-wind-speed offshore site. Finally, rotor diameter and hub height are added as design variables to assess whether the additional design degrees of freedom are significant when considering high-tip-speed designs. In each plot, the value of interest (e.g., COE) is normalized by the baseline for that particular site: an optimized design with a maximum tip speed of 80 m/s. This allows for an easy visual assessment of the relative benefits of increasing rotor tip speed. Absolute magnitudes of costs and masses are tabulated and are shown at the end of each subsection.

3.1. Benefits of Increasing Maximum Tip Speed

The first study focused on the high-wind-speed (Class IB), land-based wind site, and utilized a fixed rotor diameter. Figure 1 shows the variation in the cost of energy as a function of maximum rotor tip speed. Each point in the curve represents an optimized design. Compared to the current maximum tip speed of 80 m/s, relaxing the maximum tip-speed constraint allowed for up to a 5.4% reduction in the cost of energy. However, the marginal benefits begin to decrease at high tip speeds; increasing the tip speed beyond 110 m/s provides little to no additional benefit.

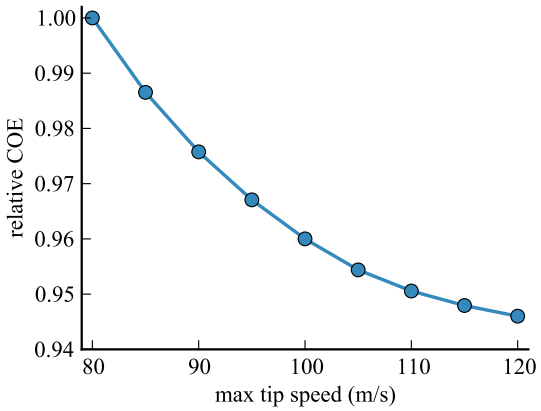

Figure 1. Cost of energy as a function of rotor tip speed for a Class IB land-based turbine design.

The decrease in the cost of energy was driven almost entirely by the decrease in turbine capital costs (Figure 2a). It was expected that the main benefit to increased tip speed would be the impact of torque load reduction on the drivetrain. There was some additional energy capture due to the more optimal tip-speed ratios near the top of Region 2; however, the corresponding change in annual energy production was extremely minimal: less than 0.5% (Figure 2b).

Of the decrease in turbine capital costs, almost all of the cost savings came from a lighter nacelle. The mass changes in the blades, nacelle, and tower are shown in Figures 3a to 3c. The nacelle was able to decrease its mass by up to 14%, whereas the blade and tower mass changed by less than 2.5% and 4.5%, respectively. Interestingly, the blade mass initially decreased slowly, but then started to increase sharply with tip speed. As the tip speeds increases, a lower blade solidity is advantageous for aerodynamic performance. However, to compensate for the smaller section chords, extra material is required in the spar-cap and trailing-edge panels

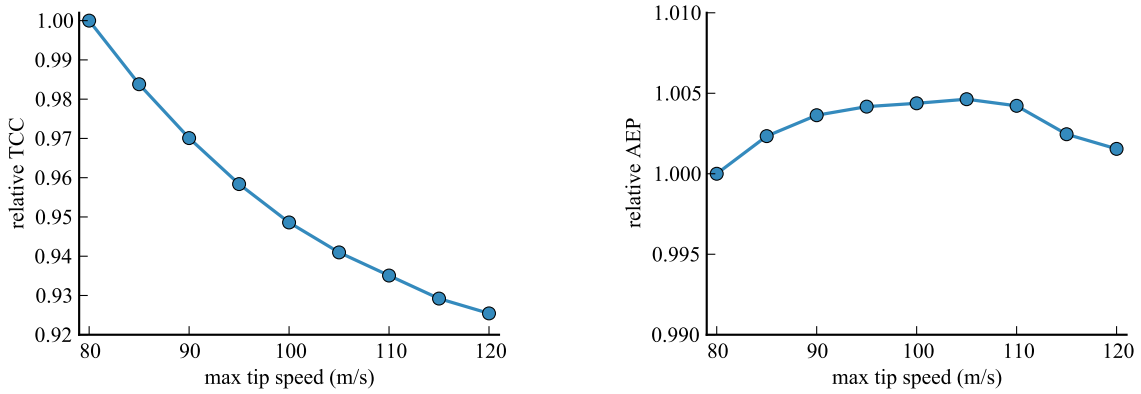

(a) Turbine capital costs

(b) Annual energy production

Figure 2. The most significant changes in the components of cost of energy were in the annual energy production and the turbine capital costs.

to meet buckling, fatigue, and deflection requirements. At high tip speeds, the increase in internal structure outweighed the decrease in mass from lower solidity, such that the optimal designs utilized slightly heavier blades. Tower mass increased throughout primarily because the increased thrust load, but in some cases the decreased margin between the first fore-aft frequency of the tower and the rotational frequency of the rotor also required a stiffer tower.

Finally, the savings in nacelle mass were caused almost entirely by decreasing gearbox weight. Figure 3d separates the gearbox weight from the rest of the nacelle. Although the mass of the other nacelle components was not precisely constant, the magnitude of their variation was much smaller and their sum was relatively constant. The gearbox design becomes lighter as the rotor rational speed increases because for a fixed power rating, the maximum torque loads decrease.

Table 3 compares absolute numbers for the NREL 5-MW reference design and some of the minimum cost-of-energy designs for the same site conditions. The reference design is not an optimized configuration and is only shown for comparison purposes. The main difference derived from optimizing the reference configuration was lighter blades and a significantly lighter tower.

Table 3. Comparison of the NREL 5-MW reference design to the minimum cost-of-energy version of that design for the same site conditions.

	Reference	Optimized	Optimized	Optimized
Max tip speed	80.0	80.0	100.0	120.0
COE (cents/kWh)	6.22	5.88	5.65	5.56
TCC ($/kW)	1,702	1,557	1,477	1,441
BOS ($/kW)	559	552	544	541
OPEX (cents/kWh)	1.22	1.22	1.22	1.22
AEP (MWh)	19,566	19,450	19,535	19,480
blade mass (kg)	17,310	14,468	14,424	14,784
nacelle mass (kg)	209,404	208,021	190,638	179,678
tower mass (kg)	349,644	254,263	259,149	264,564

3.2. Comparison Across Sites

To help assess whether or not the results of the previous section are site-specific or reflect more general trends, the same tip-speed sweep optimizations were evaluated for two additional wind sites as noted in the methodology (Section 2).

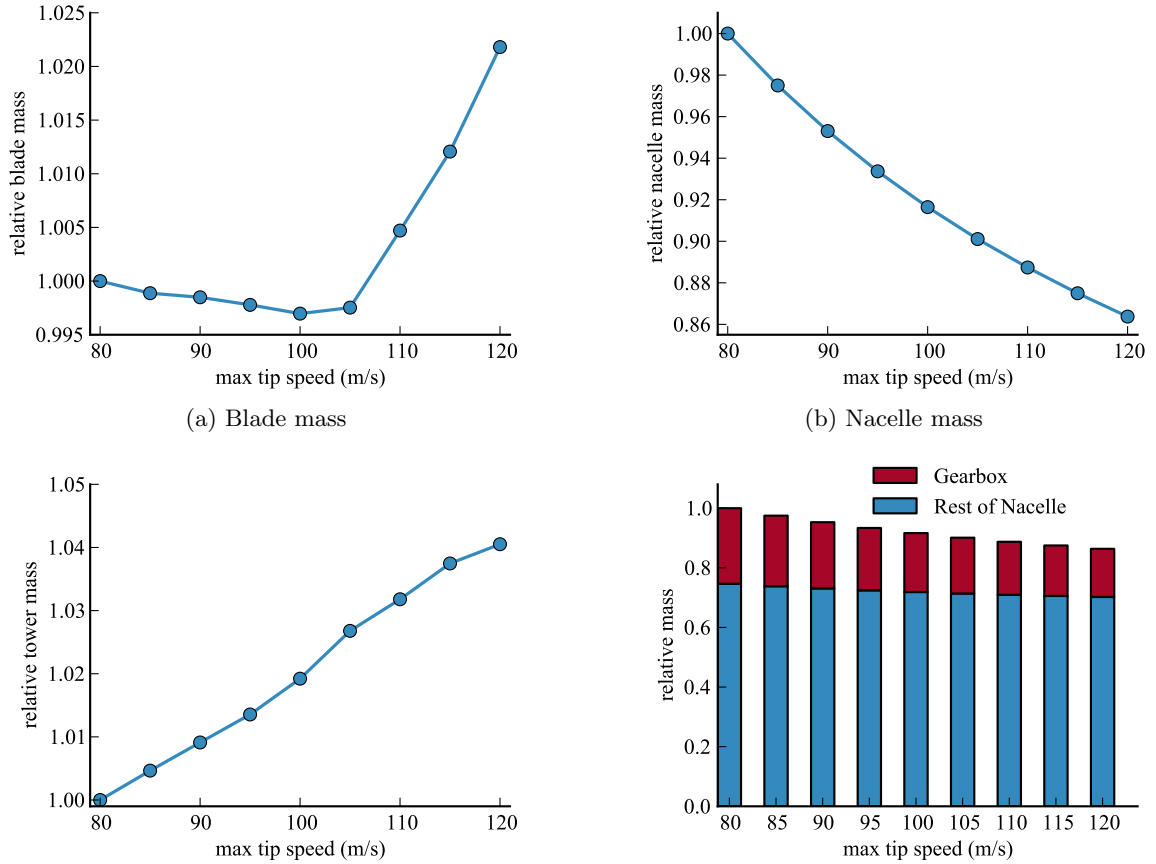

(a) Blade mass

(b) Nacelle mass

(c) Tower mass

(d) Gearbox mass and other nacelle component masses

Figure 3. Mass changes in major turbine components as the maximum allowable tip speed increased.

Figure 4 shows the performance trends for minimum cost-of-energy turbines designed for a low-wind-speed land-based site, and a high-wind-speed offshore site. The results for the high-wind-speed land-based site were shown already in Figure 1. The primary change between wind sites was a shift in the costs, with the turbines designed for the low-wind-speed Class III site having a higher cost of energy and the offshore designs having an even higher cost of energy (see Table 4). Across the sites, many of the primary conclusions were the same. Most of the benefit of higher tip speeds was realized by tip speeds of 100 m/s, and the reduced costs primarily resulted from a lighter gearbox. The cost reductions from higher tip speeds were less pronounced for the offshore case (a 2.1% maximum reduction in the cost of energy). This is because the turbine capital costs represent a smaller fraction of total costs for offshore wind turbines. Table 4 summarizes, in absolute magnitude, some of the differences in the costs and masses of the optimized designs across the three sites.

3.3. Additional Design Degrees of Freedom

For all previously presented results, the rotor diameter was held constant as the maximum tip-speed ratio was increased. This means that the rotor rotation speed could be increased as needed to decrease maximum torque loads. However, by adding rotor diameter as a design variable, additional benefits may be realized. The optimal rotor diameter is nonobvious as there are trade-offs with increased capture area but decreased maximum rotational speeds as the rotor diameter increases. Because rotor diameter was allowed to change, the hub height was also included as a design variable. A constraint was added requiring that the ground-blade

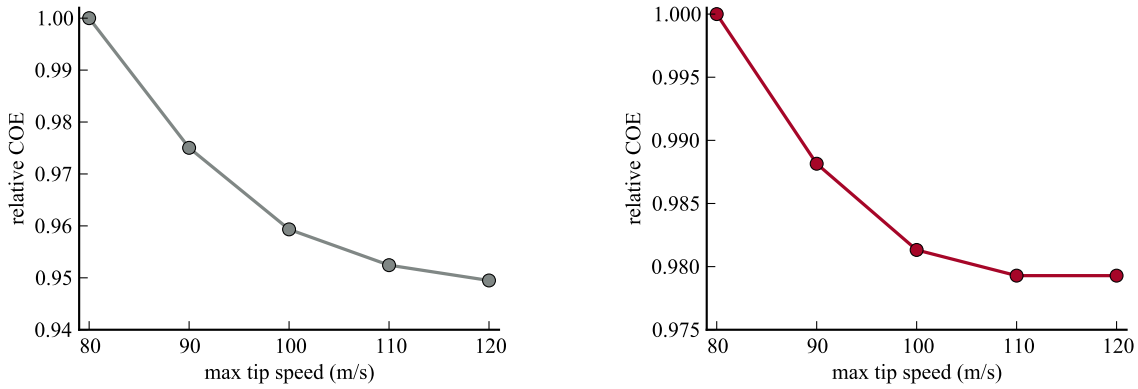

(a) Class IIIB, land-based

(b) Class IB, offshore

Figure 4. Variation in minimum cost-of-energy turbine designs for different wind sites.

Table 4. Mass and cost breakdown for minimum cost-of-energy designs at three wind sites.

	Site 1: Land IB		Site 2: Land IIIB		Site 3: Offshore IB	
Max tip speed	80.0	120.0	80.0	120.0	80.0	120.0
COE (cents/kWh)	5.88	5.56	8.40	7.98	19.92	19.51
TCC ($/kW)	1,557	1,441	1,533	1,422	1,854	1,754
BOS ($/kW)	552	541	550	539	3,825	3,818
OPEX (cents/kWh)	1.22	1.22	1.37	1.37	2.81	2.81
AEP (MWh)	19,450	19,480	13,053	13,025	19,191	19,235
blade mass (kg)	14,468	14,784	13,037	13,681	14,742	14,664
nacelle mass (kg)	208,021	179,678	208,242	179,536	207,988	186,103
tower mass (kg)	254,263	264,564	257,528	269,182	257,050	264,422
monopile mass (kg)	—	—	—	—	149,290	158,476

clearance was at least 30 m; however, this constraint was never active for any of the designs.

Figure 5a compares the minimum cost of energy for the land-based Class IB site at fixed diameter and hub height, to designs that were allowed to change diameter and hub height. To isolate the effect of tip-speed increase, the diameter and hub height were first optimized at 80 m/s and then held constant for the fixed case. For this site, the initial rotor diameter shrunk a little from the reference design (from 126 m to 120 m), and the rotor hub height increased from the reference value of 90 m to 110 m. The figure suggests that most of the benefit was simply due to optimizing the diameter and hub height initially as opposed to reoptimizing for each tip speed. The initial optimization decreased the cost of energy by approximately 0.8%, whereas reoptimizing the diameter and hub height at each tip speed yielded negligible benefit except at very high tip speeds. The optimal rotor diameter deviated very little from its initial value (Figure 5b). The hub height changed more significantly, with the tower height decreasing as the tip speed increased. As the nacelle shrunk in size at the higher tip speeds, and thrust loads increased, the cost trade-offs favored decreased AEP in exchange for a shorter tower.

The same study was repeated for the low-wind-speed land-based site, as shown in Figure 6. The initial design used a much larger optimal rotor diameter (141 m) and taller hub height (142 m) to take advantage of the low-wind-speed site. This alone reduced the cost of energy by approximately 7.5%. This simply reflects the fact that the rotor was not initially designed for a Class III site and thus was undersized for this large 5-MW machine. Again, almost all of the cost savings were due to optimizing the diameter initially. Assuming the rotor was already at the optimal diameter and hub height for an 80-m/s maximum tip speed, the impact of changing diameter and hub height with increasing maximum tip speed was small (approximately 0.23%).

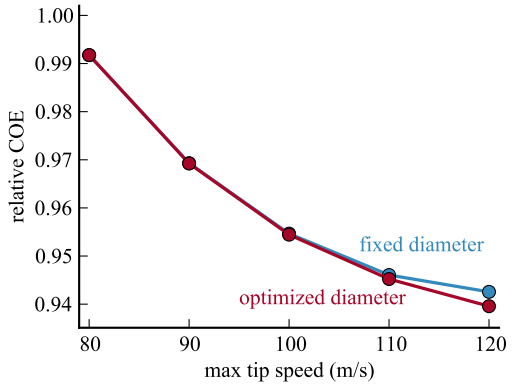

(a) Variation in cost of energy

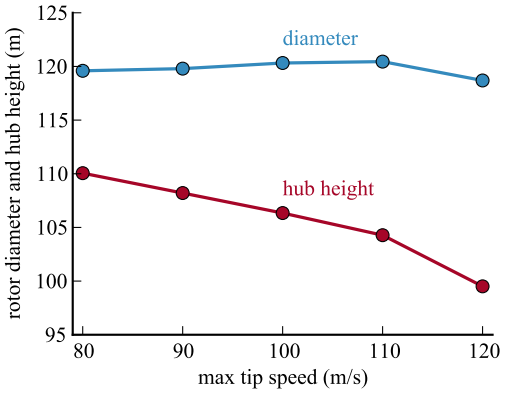

(b) Corresponding rotor diameter and hub height. Fixed values are shown by dashed lines.

Figure 5. Comparison between minimum COE designs with fixed rotor diameters and hub heights to those with optimized rotor diameters and hub heights for a Class I wind site.

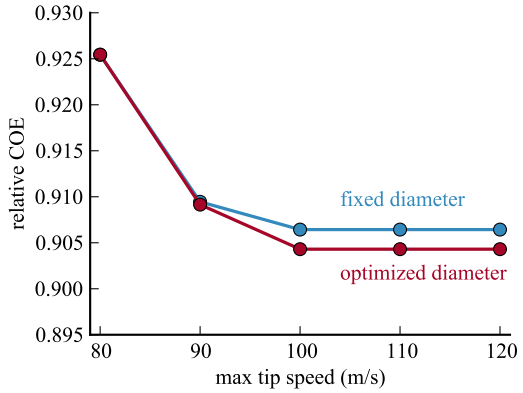

(a) Variation in cost of energy

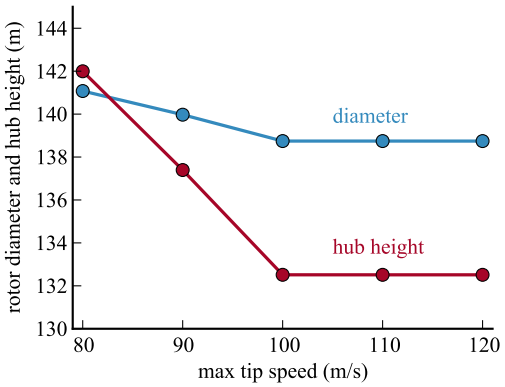

(b) Corresponding rotor diameter and hub height. Fixed values are shown by dashed lines.

Figure 6. Comparison between minimum COE designs with fixed rotor diameters and hub heights to those with optimized rotor diameters and hub heights for a Class III wind site.

4. Conclusions

This study leveraged the new WISDEM integrated wind plant software framework to better understand the system-level impacts of increasing rotor tip speed in an optimization of overall system cost of energy. Wind turbines were optimized for different maximum tip speeds to quantify the magnitude of the cost savings which may justify the research and development of novel noise-mitigation technologies. Compared to optimized wind turbines with a maximum tip speed of 80 m/s, allowing for unconstrained maximum tip speeds reduced the cost of energy by approximately 5.4% for land-based turbines and by approximately 2.1% for offshore turbines. Almost all of that benefit was due to a reduction in gearbox mass caused by the decreased maximum torque loads. Increasing the maximum tip speed to around 100-110 m/s was sufficient to realize most of the potential benefits. The same general trends in component behavior were observed for the three sites studied (land-based Class IB, offshore Class IB, and land-based Class IIIB), representing a wide spectrum of wind sites. Additional parameter variation studies found that reoptimizing the rotor diameter and hub height for each maximum tip speed did not significantly change the performance benefits, assuming that the rotor diameter and hub height were already optimal at the lower maximum tip speed. Allowing the diameter to be reoptimized as a function of tip speed yielded only an additional 0.25% savings in the cost of energy.

Areas of future work include improvements in the model fidelity, and expanding the scope of the study beyond conventional technology configurations. Improvements in the WISDEM model set, the cost models in particular, will allow for a more detailed and accurate exploration of the design trade-offs and their impact on overall cost of energy. Examining flexible downwind configurations, allowing for thicker airfoils, and testing two-bladed designs are some options that would likely yield additional performance benefits for high tip-speed rotors.

Acknowledgments

The authors gratefully thank Andy Platt of NREL for providing damage equivalent loads for the NREL 5-MW baseline design. This work was supported by the U.S. Department of Energy under Contract No. DE-AC36-08-GO28308 with the National Renewable Energy Laboratory.

References

[1] Moriarty P and Migliore P 2003 Semi-empirical aeroacoustic noise prediction code for wind turbines Tech. Rep. NREL/TP-500-34478 National Renewable Energy Laboratory Golden, CO

[2] Oerlemans S, Fisher M, Maeder T and Kögler K 2009 Reduction of wind turbine noise using optimized airfoils and trailing-edge serrations *AIAA Journal* **47** pp 1470–1481

[3] Finez A, Jacob M, Jondeau E and Roger M 2010 Broadband noise reduction with trailing edge brushes *16th AIAA/CEAS Aeroacoustics Conference*

[4] Kim T, Lee S, Kim H and Lee S 2010 Design of low noise airfoil with high aerodynamic performance for use on small wind turbines *Science in China Series E: Technological Sciences* **53** pp 75–79 ISSN 1674-7321 URL http://dx.doi.org/10.1007/s11431-009-0415-7

[5] Jamieson P 2009 Light-weight, high-speed rotors for offshore *European Offshore Wind*

[6] Resor B R, Maniaci D C, Berg J C and Richards P 2014 Effects of increasing tip velocity on wind turbine rotor design Tech. Rep. Sandia National Laboratories Albuquerque, NM (forthcoming)

[7] Dykes K, Resor B, Platt A, Guo Y, Ning A, King R, Petch D and Veers P 2014 Effect of tip speed constraints on the optimized design of a wind turbine Tech. Rep. National Renewable Energy Laboratory Golden, CO (forthcoming)

[8] Ning A, Damiani R and Moriarty P 2014 Objectives and constraints for wind turbine optimization *J. Sol. Energy Eng.* (in press)

[9] Ning A and Petch D 2014 Design optimization of downwind wind turbines *Wind Energy* (forthcoming)

[10] Dykes K, Ning A, King R, Graf P, Scott G and Veers P 2014 Sensitivity analysis of wind plant performance to key turbine design parameters: A systems engineering approach Tech. Rep. NREL/CP-5000-60920 National Renewable Energy Laboratory Golden, CO

[11] Ning A 2013 A simple solution method for the blade element momentum equations with guaranteed convergence *Wind Energy* URL http://dx.doi.org/10.1002/we.1636

[12] European Committee for Standardisation 1993 Eurocode 3: Design of steel structures—Part 1–6: General rules—Supplementary rules for the shell structures EN 1993-1-6: 20xx

[13] 2005 Guideline for the certification of offshore wind turbines Tech. Rep. IV – Part 2, Chapter 6 Germanischer Lloyd

[14] Jonkman J M and Buhl M L 2005 FAST user's guide Tech. Rep. NREL/EL-500-38230 National Renewable Energy Laboratory Golden, CO

[15] Guo Y, King R, Parsons T and Dykes K 2014 A wind turbine drivetrain sizing and optimization model set Tech. Rep. National Renewable Energy Laboratory Golden, CO (forthcoming)

[16] Tegen S, Lantz E, Hand M, Maples B, Smith A and Schwabe P 2013 2011 cost of wind energy review Tech. Rep. NREL/TP-5000-56266 National Renewable Energy Laboratory Golden, CO

[17] Fingersh L, Hand M and Laxson A 2006 Wind turbine design cost and scaling model Tech. Rep. NREL/TP-500-40566 National Renewable Energy Laboratory Golden, CO

[18] Dykes K 2014 Turbine costs SE user guide Tech. Rep. National Renewable Energy Laboratory Golden, CO (forthcoming)

[19] Gray J, Moore K T, Hearn T A and Naylor B A 2013 Standard platform for benchmarking multidisciplinary design analysis and optimization architectures *AIAA Journal* **51** pp 2380–2394 URL http://dx.doi.org/10.2514/1.J052160

[20] Gill P E, Murray W and Saunders M A 2005 SNOPT: An SQP algorithm for large-scale constrained optimization *SIAM review* **47** pp 99–131

[21] 2005 Wind turbines part 1: Design requirements Tech. Rep. IEC 61400-1 International Electrotechnical Commission

[22] Jonkman J, Butterfield S, Musial W and Scott G 2009 Definition of a 5-MW reference wind turbine for offshore system development NREL/TP-500-38060 National Renewable Energy Laboratory Golden, CO

[23] 2005 Wind turbines part 3: Design requirements for offshore wind turbines Tech. Rep. IEC 61400-3 International Electrotechnical Commission